S.-S. Li, Y.-W. Lin, Z. Ren, and C. T.-C. Nguyen, "An MSI micromechanical differential disk-array filter," *Dig. of Tech. Papers*, the 14th Int. Conf. on Solid-State Sensors & Actuators (Transducers'07), Lyon, France, June 11-14, 2007, pp. 307-311.

AN MSI MICROMECHANICAL DIFFERENTIAL DISK-ARRAY FILTER

Sheng-Shian Li[1], Yu-Wei Lin[1], Zeying Ren[1], and Clark T.-C. Nguyen[2]
[1]Dept. of Electrical Engineering & Computer Science, University of Michigan, Ann Arbor, USA
[2]Dept. of Electrical Engineering & Computer Sciences, University of California, Berkeley, USA

Abstract: A medium-scale integrated (MSI) vibrating micromechanical filter circuit that utilizes 128 radial-mode disk and mechanical link elements to achieve low motional resistance while suppressing unwanted modes and feedthrough signals has been demonstrated with a 0.06%-bandwidth insertion loss less than 2.5 dB at 163 MHz. The ability to attain an insertion loss this small *for such a tiny percent bandwidth on chip* is unprecedented and is made possible here by the availability of *Q*'s >10,000 provided by capacitively transduced resonators. In particular, the MSI mechanical circuit is able to harness the high *Q* of capacitively transduced resonators while overcoming their impedance deficiencies via strategic mechanical circuit design methodologies, such as the novel use of wavelength-optimized resonator coupling to effect a differential mode of operation that substantially improves the stopband rejection of the filter response while also suppressing unwanted modes.

Keywords: micromechanical filter, differential, array-composite, feedthrough, high-*Q*, low loss

1. INTRODUCTION

Vibrating micromechanical circuits, with their tiny size, high on-chip integration density, *Q*'s in the thousands from 1-2000 MHz [1]-[4], on/off self-switching property [5], thermal stabilities down to 18 ppm over 27-107ºC [6], and impressive aging characteristics [7], have emerged as an attractive approach for frequency generation and selection in future wireless applications. To date, capacitively transduced micromechanical circuits, such as filters [1] and mixlers [8], have been demonstrated with impressive low loss frequency characteristics; however, their sub-UHF frequencies and larger-than-conventional impedances have so far delayed deployment of these devices in conventional RF front ends. Recently, a coupled array approach that sums the outputs of numerous mechanically auto-matched resonators has been shown to lower the impedance of 68.1-MHz square-plate-array and 155-MHz disk-array filters to the point of allowing matching to a 50 Ω termination, while also exhibiting low insertion loss (*IL*) for small percent bandwidths (e.g., less than 0.28%) [9][10]. The square-plate-array filters in [9], however, are not easily scaleable to higher frequencies; meanwhile the disk-array filters in [10], although capable of attaining much higher frequencies, suffer from parasitic feedthrough currents that complicate their measurement. In addition, both filters still require termination resistors larger than 5 kΩ, thereby necessitating an L-network to impedance match to a 50 Ω antenna.

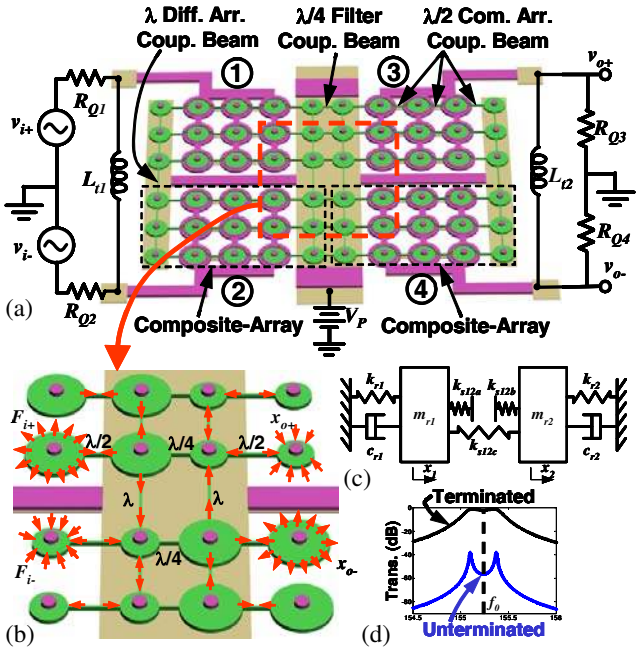

Fig. 1: (a) Perspective-view schematic, (b) 1st filter mode indicating force/displacement flows via different couplers, (c) equivalent mechanical model, and (d) terminated and unterminated frequency characteristics for a micromechanical differential disk-array filter.

Pursuant to alleviating the feedthrough and impedance issues of [10], this work employs wavelength-optimized resonator coupling to effect out-

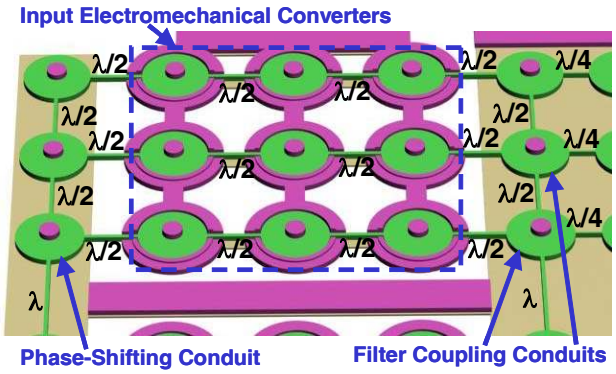

Fig. 2: Zoom-in view of the port 1 array in Fig. 1(a), indicating electromechanical converters, λ/4 filter couplers, λ/2 in-phase array couplers, and λ differential couplers.

of-phase vibrating modes among resonator-composite arrays that differentially suppress feedthrough currents from input to output, lowering the feedthrough floor by around 20 dB. By realizing such a differential design and the most complex (in terms of number of elements) hierarchical mechanical circuit to date, the 163-MHz micromechanical differential disk-array filter of this work achieves an insertion loss of 2.43 dB for 0.06% bandwidth, a 20 dB shape factor of 2.85, a designed passband ripple of less than 0.5 dB, and a stopband rejection greater than 25 dB, all with a resonator array-composite motional resistance R_x of only 977 Ω and filter termination impedances around 1.5 kΩ for each port. For comparison, a filter based on conventional SAW or FBAR technology attempting to achieve the same tiny percent bandwidth with similar termination impedance would exhibit a much worse insertion loss, typically greater than 10 dB.

2. DEVICE STRUCTURE & OPERATION

The micromechanical filter circuit of this work, shown in Fig. 1(a), comprises four disk-array composites (assigned numbers from 1 to 4), each of which contains 15 contour-mode disk resonators. As shown in Fig. 2, which zooms in on one of the arrays, these resonators are linked by λ/2 longitudinal mode array-coupling beams [10] that promote in-phase resonance among resonators in each composite array, as depicted in Fig. 1(b). This then allows summing of their motional currents to effect a lower overall impedance and higher power handling capability. In effect, via λ/2 mechanical coupling beams, each resonator array behaves like a single composite resonator with much lower impedance. As shown in Fig. 2, nine disks among each array composite are equipped with electrodes and operate as electromechanical converters to transfer energy between the electrical and mechanical domains, while other disks supply bias voltages and serve as conduits to mechanical phase-shifting links (λ) and filter coupling links (λ/4), all shown in Fig. 2. To summarize the coupling strategy, λ/2 (i.e., half-wavelength) couplers accentuate in-phase motion of disks; λ couplers force disks to mechanically vibrate out-of-phase, hence enabling differential mode operation; and λ/4 couplers spread the frequencies of the multiple-resonator system to form the bandpass response desired for the filter.

The use of λ couplers to effect differential operation is instrumental in this design, since it greatly reduces feedthrough currents (hence, improves the filter stopband rejection). This differential operation not only cancels electrical common-mode signals, but also nulls common-mode spurious vibration modes that would otherwise be generated by the overall multi-degree-of-freedom mechanical array system. The array strategy further eliminates the need for sub-micron coupling beam dimensions or notching strategies [11] that would otherwise be needed to achieve the tiny 0.06% filter bandwidth required by future RF channel-select receiver architectures [12]. This then greatly relaxes fabrication tolerances, thereby greatly enhancing control of the filter bandwidths via mere CAD layout.

Despite its complexity, the mechanical circuit of Fig. 1(a) viewed at its top hierarchical design level really boils down to the coupled two-resonator system of Fig. 1(c), with two distinct modes of vibration shown in Fig. 1(d), and two distinct mode shapes shown in Fig. 3, where the input resonator arrays (i.e., In(+) and In(-)) vibrate 180º out of phase at each mode peak, as do the output resonator arrays (i.e., Out(+) and Out(-)).

The excitation electrodes of the first and second arrays (c.f., Fig. 1(a) on the left side) comprise the differential input port of the filter, while the electrodes of the third and forth port (on the right) form the differential output configuration. To op-

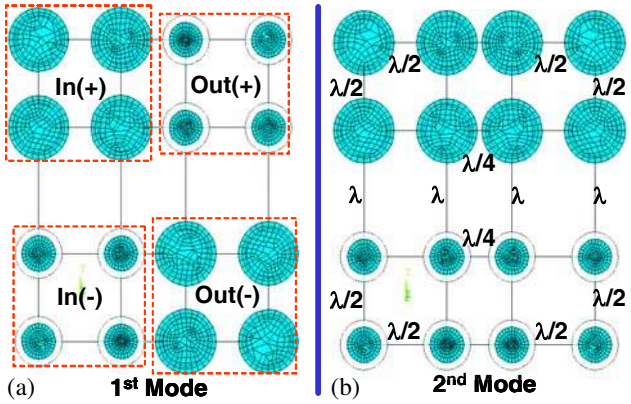

Fig. 3: Finite element simulated mode shapes for a simplified micromechanical differential contour-mode disk-array filter. (a) Out-of-phase (lower frequency) filter mode. (b) In-phase (higher frequency) filter mode.

erate this filter, a dc bias is applied to the whole filter structure via the ground plane underneath, which connects to the center stem of each disk resonator. The input ac signals v_{i+} and v_{i-} are applied through termination resistors R_{Q1} and R_{Q2} to the input electrodes of the first and second arrays, respectively. When their common frequency falls within the filter passband, the mechanical structure vibrates with an overall mode shape that combines those of Fig. 3. This creates two 180° out-of-phase motional output currents, which then generate voltages v_{o+} and v_{o-} on the R_{Q3} and R_{Q4} termination (load) resistors of the differential output electrodes in the third and fourth arrays, respectively. The differential combination of the third and forth ports (i.e., output ports) forms the desired filter passband, as depicted in Fig. 1(d).

3. ELECTRICAL EQUIVALENT CIRCUIT

Fig. 4 presents the electrical equivalent circuit of the differential disk-array filter, where two *LCR* tanks model the input (i.e., composite-array 1 and 2) and output (i.e., composite-array 3 and 4) differential resonator arrays, respectively, and a capacitive *T*-network represents the extensional quarter-wavelength coupling beams used to split the center frequency of input and output resonator arrays to form a filter passband. The figure also indicates the nodes corresponding to the electrodes and to the conductive filter structure, where the node denoting the latter is seen to provide a potential feedthrough path from input to output. From the circuit, however, one can easily surmise that when operated in a differential mode, with v_{i1}=-v_{i2}, feedthrough components flowing through C_{o1} and C_{o2} merely circulate through the differential input loop and do not enter the filter structure node. As a result, feedthrough does not reach the output, so the output ports (i.e., v_{o1} and v_{o2}) collect only motional currents. Note that the differential configuration of the output nulls common-mode feedthrough signals, as well.

It should be noted that the use of non-conductive filter coupling beams as in [8] would eliminate the feedthrough path shown in Fig. 4, thereby obviating the need for differential cancellation. However, in this case, differential operation would still be quite desirable for its equally important ability to null spurious vibration modes.

4. EXPERIMENTAL RESULTS

3μm-thick, differential disk-array filters with

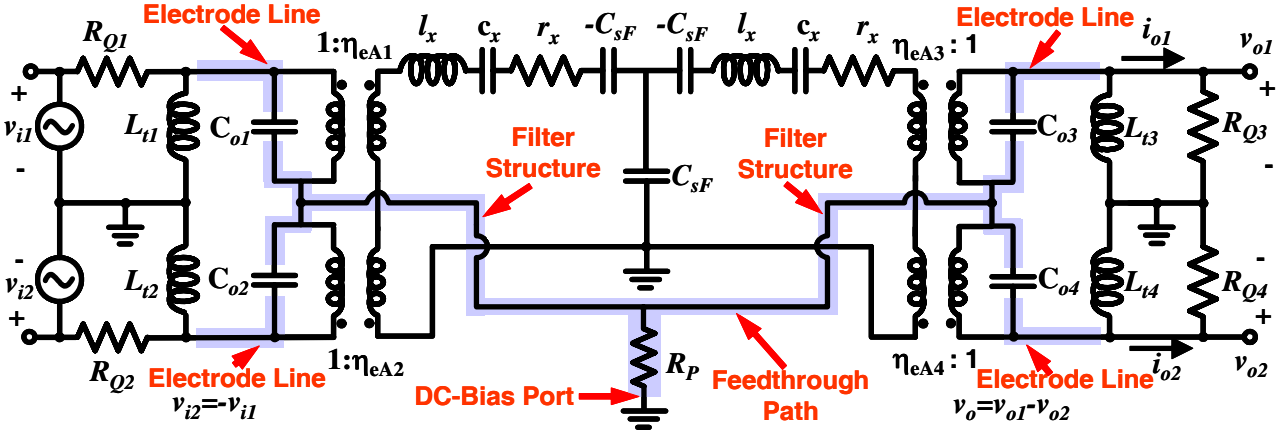

Fig. 4: Complete electrical equivalent circuit of a differential disk-array filter. Here, L_{tn}=380 nH inductors are used in the test circuit to resonate out the test board and device shunt capacitors C_{on}, where n=1, 2, 3, and 4. In a single-chip implementation, these inductors might be realized on-chip.

S.-S. Li, Y.-W. Lin, Z. Ren, and C. T.-C. Nguyen, "An MSI micromechanical differential disk-array filter," *Dig. of Tech. Papers*, the 14th Int. Conf. on Solid-State Sensors & Actuators (Transducers'07), Lyon, France, June 11-14, 2007, pp. 307-311.

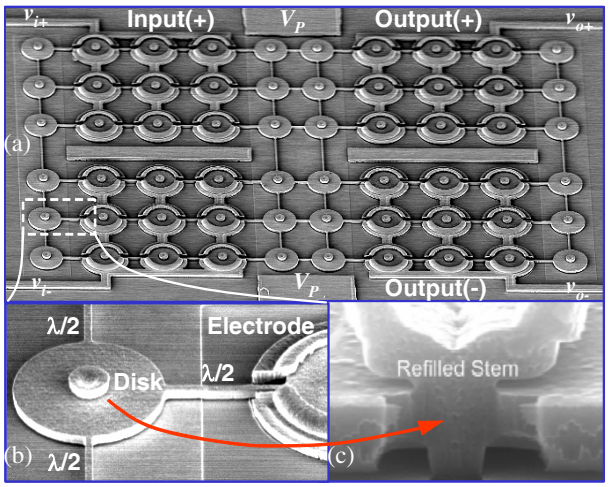

Fig. 5: (a) Top-view, (b) disk-zoomed, and (c) refilled-stem-zoomed SEM's of a polysilicon fabricated micromechanical differential disk-array filter.

80 nm electrode-to-resonator gaps were fabricated via the three-polysilicon self-aligned-and-filled stem process used previously to achieve GHz frequency disk resonators [2]. Fig. 5 presents overview and zoomed SEM's of a fabricated 163-MHz differential disk-array filter circuit.

To first gauge the degree to which feedthrough is a problem, the single-ended disk-array filter of Fig. 6(a) was also fabricated and tested, yielding the frequency response of Fig. 6(b), where large feedthrough currents nearly completely mask the motional currents of the filter. Using appropriate network analyzer measurements to de-embed the feedthrough capacitance from the spectrum [13],

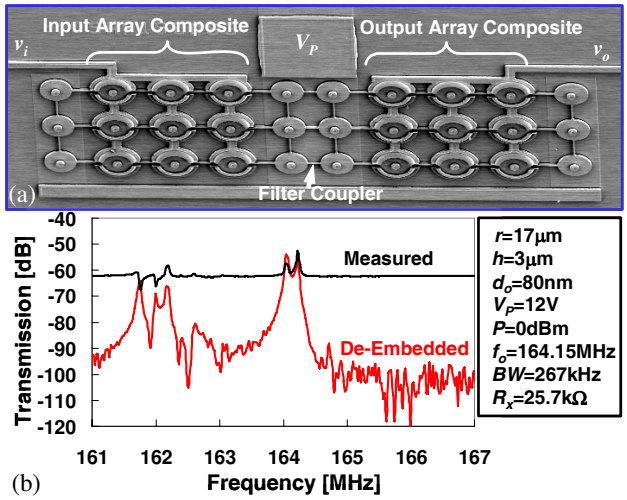

Fig. 6: (a) SEM view and (b) frequency characteristics for a fabricated single-ended (i.e., two-port) disk-array filter measured over a 6-MHz span, showing spurious modes close to desired filter passband.

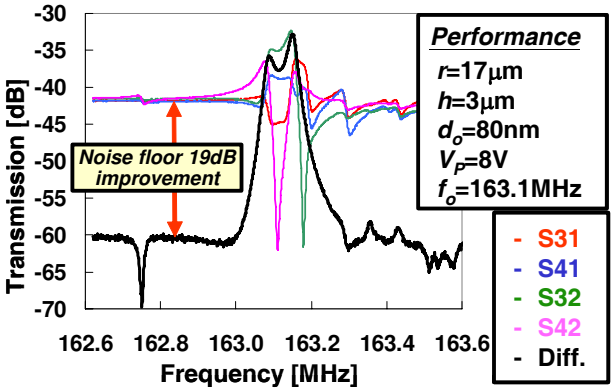

Fig. 7: Frequency characteristics for a fabricated micromechanical differential disk-array filter centered at 163.1 MHz in different testing configurations, including single ended and differential I/O. Here, S31 refers to driving at port 1 and sensing the output at port 3, and so on and so forth.

the actual filter response resulting from motional currents alone can be recovered, revealing a filter bandwidth of 267 kHz, obtained with a rather large (and perhaps impractical) filter termination resistance of 85 kΩ. Of course, de-embedding is generally not a method that would be used in an actual application, so filter performance results obtained via de-embedding are practically meaningless. (Authors publishing in the vibrating RF MEMS area are encouraged to refrain from de-embedding, or at least indicate when it is being done, so readers can correctly interpret the data. Here, it is done only to clarify feedthrough issues.) Aside from feedthrough issues, Fig. 6(b) shows that the single-ended filter further suffers from several spurious modes that arise from the complexity of the mechanical system and that creep into the neighborhood of the desired passband, crippling the ability of the structure to perform as a frequency filter.

Moving now to the differential design of

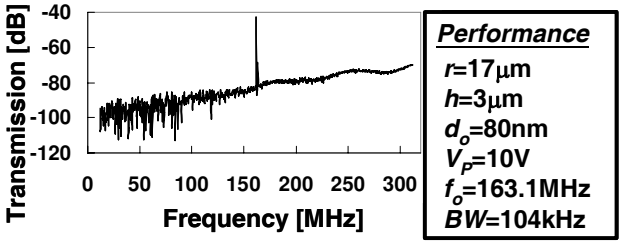

Fig. 8: Frequency characteristic for a fabricated micromechanical differential disk-array filter centered at 163.1 MHz over a 300 MHz measurement span, showing no spurious modes.

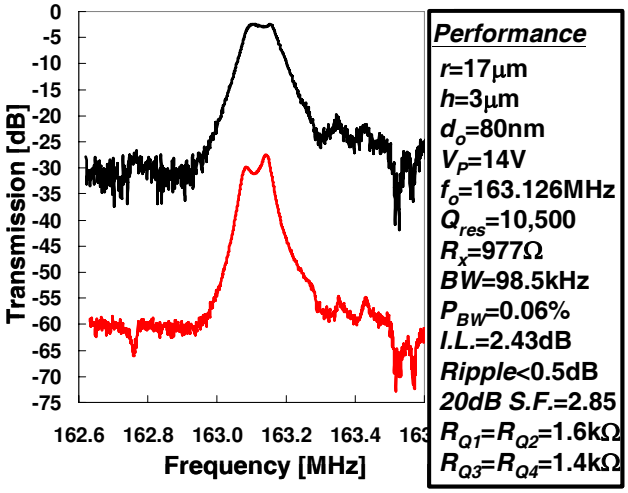

Fig. 9: Unterminated and terminated spectra for a fabricated micromechanical differential disk-array filter tested in vacuum.

Fig. 1(a), Fig. 7 compares measured singled-ended (i.e., S31, S41, S32, and S42 where 1, 2, 3, and 4 represent port 1, 2, 3, and 4, respectively, in Fig. 1(a)) and differential frequency characteristics, all now *without* any de-embedding. Here, only the differential mode spectrum resembles the desired filter response, verifying the utility of differential mode operation in suppressing feedthrough and close-in spurious modes.

Fig. 8 presents an unterminated differential mode frequency characteristic for the mechanical circuit of Fig. 1(a) measured over a wide 300-MHz span, showing no spurious modes, thereby verifying the utility of differential operation combined with strategic geometrical placement [10] for nulling even distant undesired modes.

Fig. 9 finally presents the *terminated* frequency characteristic tested in a 200-μTorr vacuum environment for the 163.1 MHz filter circuit, exhibiting the aforementioned performance, with an insertion loss of only 2.43 dB for a 0.06% bandwidth, passband ripple less than 0.5 dB, 20 dB shape factor of 2.85, while using termination resistors averaging only 1.5 kΩ. Again, the ability to attain an insertion loss this low for such a tiny percent bandwidth is made possible mainly by the sheer Q (greater than 10,000) of the constituent capacitively transduced micromechanical resonators. Since VHF disk resonators retain high Q (near 10,000) in air [2], the measured insertion loss of this 0.06% bandwidth filter is still less than 4 dB even when operated in air.

5. CONCLUSIONS

A medium-scale integrated (MSI) vibrating micromechanical filter that utilizes the most complex hierarchical mechanical circuit to date to achieve low motional resistance while suppressing unwanted modes and feedthrough signals has been demonstrated at 163 MHz with a 0.06% bandwidth insertion loss appropriate for the future RF channel-select applications targeted by this technology [12]. Aside from sheer performance, perhaps the most significant attribute of this work is the demonstration that mechanical circuit design methodologies can be just as powerful as those used in the transistor world to enhance functionality via a hierarchical building block approach.

Acknowledgments. This work was supported by DARPA and an NSF ERC on Wireless Integrated Microsystems.

References.

[1] F. D. Bannon, *et al.*, "High-Q HF …," *IEEE J. Solid-State Circuits*, vol. 35, no. 4, pp. 512-526, April 2000.

[2] J. Wang, *et al.*, "1.156-GHz …," *IEEE Trans. Ultrason., Ferroelect., Freq. Contr.*, vol. 51, pp. 1607-1628, Dec. 2004.

[3] S.-S. Li, *et al.*, "Micromechanical "hollow-disk" …," *Technical Digest*, MEMS'04, pp. 821-824.

[4] G. Piazza, *et al.*, "Low motional resistance …," *Technical Digest*, MEMS'05, pp. 20-23.

[5] S.-S. Li, *et al.*, "Self-switching vibrating …," *Proceedings*, Joint IEEE Int. Frequency Control/Precision Time & Time Interval Symposium, Vancouver, Canada, Aug. 29-31, 2005, pp. 135-141.

[6] W.-T. Hsu, *et al.*, "Stiffness-compensated …," *Technical Digest*, MEMS'02, pp. 731-734.

[7] B. Kim, *et al.*, "Frequency stability …," *Dig. of Tech. Papers*, Transducers'05, pp. 1965-1968.

[8] A.-C. Wong, *et al.*, "Micromechanical mixer-filters …," *IEEE/ASME J. Microelectromech. Syst.*, vol. 13, no. 1, pp. 100-112, Feb. 2004.

[9] M. U. Demirci, *et al.*, "A low impedance …," *Dig. of Tech. Papers*, Transducers'05, pp. 2131-2134.

[10] S.-S. Li, *et al.* "Disk-array design …," *Tech. Digest*, MEMS'06, pp. 866-869.

[11] S.-S. Li, *et al.*, "Small percent bandwidth …," *Proceedings*, 2005 IEEE Int. Ultrasonics Symposium, pp. 1295-1298.

[12] C. T.-C. Nguyen, "MEMS technology for …," *IEEE Trans. Ultrason., Ferroelect., Freq. Contr.*, vol. 54, no. 2, pp. 251-270, Feb. 2007.

[13] S.-S. Li, Thesis, University of Michigan, 2007.